



Published in final edited form as:

*Cardiovasc Eng Technol.* 2014 March 1; 5(1): 70–81. doi:10.1007/s13239-013-0171-5.

## Hemocompatibility and Hemodynamics of Novel Hyaluronan–Polyethylene Materials for Flexible Heart Valve Leaflets

David A. Prawel<sup>1,2</sup>, Harold Dean<sup>1</sup>, Marcio Forleo<sup>2</sup>, Nicole Lewis<sup>2</sup>, Justin Gangwish<sup>3</sup>, Ketul C. Popat<sup>1,2</sup>, Lakshmi Prasad DASI<sup>1,2</sup>, and Susan P. James<sup>1,2</sup>

<sup>1</sup>Department of Mechanical Engineering, Colorado State University, Fort Collins, CO, USA

<sup>2</sup>School of Biomedical Engineering, Colorado State University, Fort Collins, CO, USA

<sup>3</sup>Department of Chemical and Biological Engineering, Colorado State University, Fort Collins, CO, USA

### Abstract

Polymeric heart valves (PHVs) hold the promise to be more durable than bioprosthetic heart valves and less thrombogenic than mechanical heart valves. We introduce a new framework to manufacture hemocompatible polymeric leaflets for HV (PHV) applications using a novel material comprised of interpenetrating networks (IPNs) of hyaluronan (HA) and linear low density polyethylene (LLDPE). We establish and characterize the feasibility of the material as a substitute leaflet material through basic hemodynamic measurements in a trileaflet configuration, in addition to demonstrating superior platelet response and clotting characteristics. Plain LLDPE sheets were swollen in a solution of silylated-HA, the silylated-HA was then crosslinked to itself before it was reverted back to native HA *via* hydrolysis. Leaflets were characterized with respect to (1) bending stiffness, (2) hydrophilicity, (3) whole blood clotting, and (4) cell (platelet and leukocyte) adhesion under static conditions using fresh human blood. *In vitro* hemodynamic testing of prototype HA/LLDPE IPN PHVs was used to assess feasibility as functional HVs. Bending stiffness was not significantly different from natural fresh leaflets. HA/LLDPE IPNs were more hydrophilic than LLDPE controls. HA/LLDPE IPNs caused less whole blood clotting and reduced cell adhesion compared to the plain LLDPE control. Prototype PHVs made with HA/LLDPE IPNs demonstrated an acceptable regurgitation fraction of  $4.77 \pm 0.42\%$ , and effective orifice area in the range  $2.34 \pm 0.5 \text{ cm}^2$ . These results demonstrate strong potential for IPNs between HA and polymers as future hemocompatible HV leaflets. Further studies are necessary to assess durability and calcification resistance.

### Keywords

Interpenetrating polymer network; Hemocompatible; Thrombus; Blood-contacting materials; Hemodynamics; Platelet; Bending stiffness

---

© 2013 Biomedical Engineering Society

Address correspondence to Susan P. James, Department of Mechanical Engineering, Colorado State University, Fort Collins, CO, USA. Susan.James@colostate.edu.

### CONFLICT OF INTEREST

Authors David A. Prawel, Harold (Casey) Dean, Marcio Forleo, Nicole Lewis, Justin Gangwish, Ketul C. Popat, Lakshmi Prasad Dasi, and Susan P. James declare that they have no conflict of interest.

## INTRODUCTION

Artificial heart valves (HVs) have extended the lives of countless people suffering from HV diseases. Currently, over 290,000 HV procedures are performed annually worldwide, and that number is estimated to triple to over 850,000 by 2050,<sup>27,40</sup> increasing at a rate of 5–12% per year.<sup>6,8</sup> Despite their widespread use, complications include structural valvular deterioration, non-structural dysfunction, valve thrombosis, embolism, bleeding, and endocarditis.<sup>11,29</sup> Zilla *et al.*'s review<sup>45</sup> of the current status of the field finds that “prosthetic HVs epitomize both the triumphant advance of cardiac surgery in its early days and its stagnation into a retrospective, exclusive first world discipline of late”. Indeed, advancements in either mechanical or bioprosthetic design since the 1960–1970s have been incremental. The most promising recent advancement, catheter-delivered prostheses, relies on tissue valves with unacceptable durability, especially for young HV patients.<sup>35</sup>

In contrast to stented and non-stented trileaflet valves with flexible leaflets and superior hemodynamics, mechanical heart valves (MHVs) fail primarily due to thrombosis which obstructs leaflet motion.<sup>4,13,30</sup> For this reason, anticoagulation needs to be robust for MHVs. A durable, polymeric heart valves (PHV) that mimics the superior design characteristics of stented trileaflet valves, even with far less aggressive anticoagulation therapy, has the potential to offset the use of MHVs, whose main drawbacks are secondary to the aggressive anticoagulation requirements. An argument in favor of synthetic PHVs is that they don't require as much anticoagulation therapy as MHVs due to superior hemodynamics, reduced calcification, and because their failure mode is not catastrophic. If this is true, PHVs would also offer a significant advantage over tissue-based heart valves (THVs).

Indeed, since the first polyurethane, flexible-leaflet PHVs were implanted in the 1960s, synthetic PHVs have attempted to combine the durability of mechanical valves with the hemocompatibility of THVs. Unfortunately, this has not been the case—to date there are no clinically acceptable PHVs beyond those used short-term in artificial hearts.<sup>16,45</sup> Although polyurethane HVs exhibit acceptable short-term mechanical properties and performance, their susceptibility to hydrolytic and oxidative biodegradation and subsequent mechanical failure has limited their successful use. Furthermore, while flexible leaf-lets provide more natural hemodynamics,<sup>25</sup> thrombus formation remains a high risk because the polymers most often used are inherently thrombogenic, and in some cases exhibit a tendency to calcify *in vivo*.<sup>16</sup> Work has continued with flexible polymeric valves based on polyurethane chemistry. Daebritz *et al.*'s polycarbonateurethane valves (ADIAM Life Science AG, Erkelenz, Germany) were developed to optimize hemodynamics and increase durability. However, the material was not specifically designed to avoid calcification. The literature suggests that material surface properties (particularly hydrophilicity), in addition to natural hemodynamics are vital to avoid calcification. Indeed, in two *in vivo* animal studies using the ADIAM valve (one aortic and one mitral) the explanted valves showed some calcification, albeit less than control tissue valves.<sup>9,10</sup> Although the authors did not study the surface characteristics, it is likely these materials are at least as hydrophobic as their polyurethane predecessors (nothing was reported that might change it), raising concerns about their long-term resistance to calcification. Kidane *et al.* recently developed flexible PHVs with leaflets made from a 2% polyhedral oligomeric silsesquioxane-poly(carbonate-urea) urethane (POSS-PCU). These exhibit good mechanical properties due to the addition of POSS. However, both PCU alone and POSS-PCU are hydrophobic, with POSS-PCU exhibiting the highest water contact angles of the two materials.<sup>22</sup> *In vitro* calcification tests showed some calcification and *in vivo* performance is unknown.<sup>15</sup>

Several researchers have considered surface coatings on hydrophobic synthetic polymers to enhance performance. While none of these has yet to lead to a clinically successful

polymeric leaflet valve, these studies have demonstrated that surface hydrophilicity and charge affect the propensity for thrombogenesis and calcification.<sup>19,28</sup> Glycosylated surfaces may mimic the biochemical activity of the glycocalyx of the blood vessel lumen, which presents heparin-like glycosaminoglycans (GAGs).<sup>7,39</sup> GAGs such as heparin are widely known to improve hemocompatibility of surfaces.<sup>5,32,33</sup> Coatings based on hyaluronan (HA) and chondroitin sulfate, other broadly studied GAGs, have been shown to reduce platelet adhesion in small diameter vascular grafts.<sup>23</sup> Other studies have shown that HA and other GAGs help mitigate calcification in bioprosthetic materials.<sup>21</sup>

HA is a naturally occurring polysaccharide that has a large unbranched structure consisting of repeating disaccharides of *N*-acetylglucosamine and glucuronic acid making it very hydrophilic and anionic. HA is present in all vertebrate tissues and body fluids with relatively high concentrations in native HV leaflets, particularly those regions of the valve subject to compression.<sup>18,21</sup> Earlier work developed a novel synthesis process for creating interpenetrating networks (IPNs) between hydrophilic polysaccharides (e.g., HA) and hydrophobic synthetic polymers (e.g., polyethylene).<sup>20</sup> This process augments the strength and durability of the synthetic plastic with the added biocompatibility and hydrophilicity of HA. Biomaterials made from ultra-high molecular weight polyethylene (UHMWPE) and HA using this novel process are currently in commercial use in the EU in a partial resurfacing knee implant system called BioPoly®.<sup>21,43</sup> This enhanced polymer is highly hydrophilic, with the strength and durability of UHMWPE.<sup>42,44</sup> *In vitro* hip simulator tests to 5 million cycles and *in vivo* (goat knee) studies to 12 months have shown BioPoly implants to be very durable—with no signs of wear, mechanical deterioration, calcification or HA loss.<sup>21</sup>

The long-term goal of this study is to develop HA-enhanced synthetic polymers for blood-contacting applications, such as flexible PHV leaflets engineered specifically to address the known drawbacks of THVs and MHVs. It is hypothesized that the base material and manufacturing process can be optimized to result in low bending stiffness, high strength HA/polyethylene IPN materials that will result in less thrombus formation and platelet adhesion than plain polyethylene and THV materials. In particular, this paper examines the use of linear low density polyethylene (LLDPE) as the base material for flexible heart valve leaflets in a trileaflet HV. LLDPE was selected for its high tensile and tear strengths and relatively low bending stiffness.<sup>26</sup> The objectives of this paper are to: (1) demonstrate the manufacturability of HA/LLDPE IPNs while controlling percent crystallinity, mechanical properties and HA content; (2) establish and characterize the feasibility of the material as a substitute leaflet material through basic hemodynamic measurements in a trileaflet configuration; (3) quantify the hydrophilicity, thrombogenicity, and propensity for platelet adhesion and activation with the HA/LLDPE IPN materials; and (4) evaluate hemodynamic performance with HA/LLDPE IPN materials as valve leaflets.

## MATERIALS AND METHODS

### Manufacturing the HA/LLDPE IPN Materials as Leaflet Substitute

Preliminary studies examined LLDPE blown films made from three different Dowlex resins (2344, 2056 and 2036G; Dow Chemical Company, Edegem, Belgium) for their amenability to the swelling process used to manufacture the HA/LLDPE IPN materials. Dowlex 2056 was chosen for its high degree of swelling, high yield, tensile and tear strengths, and relatively low tensile and bending moduli.<sup>12</sup> LLDPE films were blow molded by Flex-Pack Engineering, Inc. (Union-town, OH) from Dowlex 2056 resin (3 cm × 3 cm with nominal thickness 0.05 mm, measured average thickness 0.08 mm, melt index 1.0 g/10 min, density 0.920 g/cm<sup>3</sup>, and nascent crystallinity 28.71 ± 2.14%). All films were blown without filler

and with no additional surface treatment. All test samples were punched (8 mm, round) from HA/LLDPE film manufactured using the parameters shown in Table 1.

HA/LLDPE IPN materials were manufactured using the swelling method described in detail elsewhere.<sup>12,20,42</sup> Briefly, sodium HA (~700 kDa, Lifecore Biomedical) was complexed with cetyltrimethylammonium (CTA) bromide to create HA-CTA, which was then silylated to create silylHA-CTA. The hydrophobic silylHA-CTA was introduced into the hydrophobic host (LLDPE) *via* swelling for 60 min in a hot (50 °C) silylHA-CTA/xylene solution. The aforementioned preliminary studies explored a variety of swelling temperatures and times; swelling at 50 °C for 60 min maximized swelling (and thus the introduction of silylHA-CTA) while minimizing increases in percent crystallinity ( $\%X_c$ ), thus minimizing undesirable increases in elastic modulus. Three different silylHA-CTA/xylene concentrations were used for swelling (5, 15, and 25 mg/mL) in an effort to get final materials with different and increasing HA contents.

The silylHA-CTA introduced into the LLDPE films was crosslinked with a 2% (v/v) poly(hexamethylene diisocyanate) (HMDI) xylenes solution. Treated LLDPE films were swelled at 50 °C in a 2% (v/v) HMDI xylenes solution (i.e., HA crosslinking solution) for 60 min, and the crosslinker was cured in a vacuum oven at 50 °C for 3 h. Treated samples were then washed with acetone to remove excess HMDI and vacuum dried at room temperature until no change in weight was observed.

Because the silylHA-CTA was entangled at the molecular level and then crosslinked, the IPN survives hydrolysis (which converts the hydrophobic silylHA-CTA back into hydrophilic HA); i.e., the resulting hydrophilic HA cannot phase separate from the hydrophobic LLDPE. The details of hydrolysis are described in detail elsewhere.<sup>44</sup> Briefly, hydrolysis was performed by three successive 60 min ultrasonic baths in 0.2 M NaCl solution (H<sub>2</sub>O:ethyl alcohol, 1:1) at 45 °C, followed by 60 min of additional ultrasonication in pure 0.2 M NaCl aqueous solution without ethyl alcohol, then washed twice in 3:2 H<sub>2</sub>O:ethyl alcohol solutions (first 2 h, then 30 min), then dehydrated in acetone for 60 min, and finally dried under vacuum at 50 °C until no change in weight was observed.

Half of the samples then received a final surface coating of HA by dipping in a 1% (w/v) aqueous HA solution, drying, and then crosslinking with a 2% (v/v) HMDI xylenes solution, followed by curing in a vacuum oven for 3 h at 50 °C and subsequent washing in acetone.

### Percent Crystallinity Measurement

The effects of the swelling manufacturing treatment on percent crystallinity and mechanical properties of the HA/LLDPE IPNs relative to unmodified LLDPE were also examined. Percent crystallinity was measured by means of a TA Instruments differential scanning calorimeter (DSC) 2920 in a dry N<sub>2</sub> atmosphere in accordance with ASTM standard D3418-12.<sup>3</sup> Samples were heated from 24 to 180 °C at a rate of 10 °C/min, and held at equilibrium for 1 min (all with N<sub>2</sub> atmosphere). The  $\%X_c$  of the sample was calculated by dividing the heat of fusion ( $H_f$ ) of the sample by 288 J/g<sup>24,37</sup> based on base polymer (because the 100% crystalline  $H_f$  of HA/LLDPE IPN is unknown) and multiplying by 100. All reported average values and standard deviation for  $\%X_c$  were calculated from a sample size of three per treatment group.

### Mechanical Testing

ASTM D882-12 standard<sup>2</sup> tensile test specimens were stamped out of HA/LLDPE IPN films. An electromechanical Tinius Olsen UTM axial test system (Horsham, PA) was used in conjunction with Test Navigator software (Tinius Olsen) to perform all tensile tests. A

uniaxial (tension/compression) 1000 N load cell (Model H1K-S) was used. All samples were placed in de-ionized water (DIH<sub>2</sub>O) for 60 min, allowing the HA to hydrate prior to testing. Elongation data was calculated from crosshead data (the change in gage length was divided by the original gage length of the sample, as specified in the standard).

The ASTM D1388-08 testing standard<sup>1</sup> was used to determine the bending modulus of the samples. Bending specimens were stamped out of HA/LLDPE IPN films and a Shirley Stiffness Tester (Model M003B) was used. One sample of each treatment group was used at both ends, on opposite faces for a total of four measurements per sample group. The samples were exposed to the standard atmosphere for conditioning for at least 24 h or until the mass of the specimen did not change by more than 0.25% in 2 h intervals. Samples were then placed in DIH<sub>2</sub>O for 60 min, allowing the HA to hydrate. Specimens were slid at a uniform rate until the bending length was determined. This was used to calculate the flexural rigidity  $G$  (mg.cm):

$$G=0.10MC^3,$$

where  $M$  is the mass per unit area (g/m<sup>2</sup>) and  $C$  the bending length (cm);

The bending modulus  $K$  (kg/cm<sup>2</sup>) is then given by the following formula:

$$K=\frac{12G \times 10^{-6}}{t^3}$$

where  $G$  is the flexural rigidity (mg cm) and  $t$  the sample thickness (cm).

Bending stiffness was approximated by first measuring the bending length, thickness, and mass per unit area of the samples, from which flexural rigidity was calculated, which was then used to calculate the bending modulus. This bending modulus was multiplied by the moment of inertia about the bending axis for each sample, which was approximated from measured dimensions, resulting in an approximate bending stiffness.

The composition of the samples was determined using a TA Instruments thermal gravimetric analyzer (TGA) 2950 at a heating rate of 10 °C/min in helium. Masses of individual specimens ranged from 5 to 15 mg.

Static water contact angles were measured on all samples using the sessile drop method with a Krüss DSA 10 goniometer (KR SS GmbH, Hamburg, Germany). Briefly, a 3 μL DIH<sub>2</sub>O drop was applied to the sample surface at room temperature and contact angles were immediately measured using a circular fitting profile.

### Hemocompatibility: In Vitro Whole Blood Clotting on LLDPE Films

The interaction of LLDPE and HA/LLDPE films with whole blood was investigated to evaluate their thrombogenic properties using methods described previously.<sup>31</sup> Briefly, whole blood was acquired by venipuncture from healthy non-medicated adults into centrifuge tubes, under an approved institutional IRB protocol. The first 6 mL was discarded to prevent contamination from tissue thromboplastin activated by the needle puncture. Five μL of blood was immediately dropped onto LLDPE samples and controls in a well plate. At 30 and 60 min time points, samples were placed into a secondary sterile well plate containing 500 μL of DIH<sub>2</sub>O. Special care was taken to prevent disturbing the blood droplet. Well plates were gently agitated (manually) for 30 s and held stationary in DIH<sub>2</sub>O for 5 min at

room temperature to allow release of free hemoglobin from red blood cells that were not trapped in a thrombus. Samples were then removed from the well plates and placed in a dry, sterile well plate to be processed for scanning electron microscopy (SEM). Two hundred  $\mu\text{L}$  of the remaining water/blood mixture from each well was placed into a new well plate for measurement of the absorbance (at 540 nm) of free hemoglobin using a BMG Labtech FLOUstar Omega plate reader. The concentration of free hemoglobin in solution is directly proportional to the absorbance value.

HA/LLDPE + 1.0% HA and LLDPE-Reference samples were fixed using the method described below, coated with 10 nm of gold and imaged (15.0 keV) using SEM (JOEL JSM-6500F, Tokyo, Japan). Prepared specimens were stored in a vacuum oven at room temperature prior to imaging.

### **Hemocompatibility: Cell Adhesion, Morphology and Activation**

HA-treated and untreated samples ( $n = 3$ ) were used for evaluation of cell adhesion, morphology and activation. Briefly, whole blood was acquired by venipuncture from healthy non-medicated adults, and collected into 6 mL vacuum tubes coated with ethylenediamine tetra acetic acid (EDTA) as an anticoagulant. The first 6 mL was discarded to prevent contamination from tissue thromboplastin activated by the needle puncture. Blood vials were centrifuged at  $150\times g$  for 15 min, then plasma was pooled into a fresh tube and used within 2 h of collection.

HA/LLDPE + 1.0% HA and LLDPE-Reference samples (round, 4.8 mm diameter) were bathed in  $\text{DIH}_2\text{O}$  for 12–14 h, then sterilized by 30 min UV exposure and rinsed in phosphate-buffered saline (PBS). Samples were then incubated in pooled plasma (250  $\mu\text{L}$ ) on a shaker plate (100 rpm) at room temperature for 2 h, prior to evaluation of cell adhesion, morphology and activation.

Cell adhesion was assessed using calcein-AM live stain (Invitrogen). Following incubation, plasma was aspirated and samples were rinsed twice with PBS to remove non-adherent cells. Samples (3 per treatment group) were transferred to a new, sterile well plate and incubated in darkness in 500  $\mu\text{L}$  of 5  $\mu\text{M}$  calcein-AM solution at room temperature for 20 min. Samples were then rinsed in PBS and imaged using a fluorescence microscope (Zeiss) with filter set 62 HE BP 474/28 (green). Three images per sample were obtained. Cell adhesion was determined from resulting fluorescent images using ImageJ software.

Platelet morphology and activation was assessed using SEM. After sample incubation in plasma for 2 h, samples (2 per treatment group) were bathed in a primary fixative [6% glutaraldehyde (Sigma), 0.1 M sodium cacodylate (Alfa Aesar), and 0.1 M sucrose (Sigma)] for 45 min, then in a buffer solution (primary fixative without glutaraldehyde) for 2 h, followed by consecutive 35, 50, 70, and 100% ethanol baths for 10 min each. Samples were air dried and stored in a vacuum desiccator at room temperature prior to imaging. Samples were gold-coated (10 nm) and imaged at 15 kV. The number of unactivated and activated platelets was counted from 5 images per treatment group, using ImageJ software. These counts were averaged for each treatment group, and the number of cells per  $\text{mm}^2$  and standard deviations were then calculated.

### **Valve Leaflet Test Bed**

To test the various leaflet material compositions, a snap-on leaflet test bed was designed based on the geometry of a 25 mm Carpentier-Edwards PERI-MOUNT Aortic Heart Valve. The snap-on leaflet test bed was built using a Stratasys 3D printer (Stratasys uPrint, Eden Prairie, MN) using acrylonitrile butadiene styrene (ABS) plastic and is made up of three

pieces: an inner stent and two outer stents (refer to Fig. 1). The inner stent provides structural support for the leaflet sample while the two outer stents hold both the leaflets in position and the valve inside the valve chamber.

The test bed valve was designed parametrically using SolidWorks software (Dassault Systèmes, Vélizy-Villacoublay, France) such that it would fit the valve chamber of the pulsatile flow loop, and to allow different leaflet materials to be easily exchanged for testing. The overall aspect ratio of the test bed valve, defined as the ratio of the height of the stent post (10.3 mm) to the inner diameter of the valve annulus (19.7 mm), is 0.52 which governs the stent profile.

### In Vitro Pulsatile Flow Loop Testing

Trileaflet HVs made from sheets of LLDPE-Reference, LLDPE + 1.0% HA, LLDPE + 1.5% HA, HA/LLDPE + 0.5% HA + SD, LLDPE + 1.5% HA + SD, and samples were tested *in vitro* to assess basic hemodynamic competence of the valves using the above test bed. An *in vitro* pulsatile flow loop<sup>14</sup> similar to one described in Leo *et al.*<sup>25</sup> was used to reproduce physiological aortic flow conditions through trileaflet valves made with HA/LLDPE IPN flexible leaflets in the aortic position. The valve was subjected to the following hemodynamic conditions: cardiac output of 5 LPM; systolic fraction of 33%, and mean aortic pressure of approximately 100 mm Hg. The heart rate was set at 60 bpm. Measurements included high-speed videos of the valve leaflet motion, instantaneous aortic flow rate, and instantaneous pressure upstream and downstream of the valve throughout the cardiac cycle. Flow and pressure measurements were done for a total of 20 heart beats. These hemodynamic measurements enabled the calculation of valve regurgitant volume, defined as the regurgitant volume and effective orifice area (EOA), using the Gorlin equation.<sup>41</sup> These data were compared between treatments, as well as to data points of numerous other clinical prosthetic valves.<sup>41</sup>

### Statistics

Statistics were analyzed using SigmaStat software (Systat Software Inc.; Richmond, CA) and SAS (Cary, NC). A single-factor ANOVA test with a 95% confidence interval was performed; multiple comparisons were performed *via* the Holm-Sidak method when sample population standard deviations and population sample sizes were similar.

## RESULTS

### Mechanical Testing

Table 1 indicates the range of HA compositions (from 0.5 to 1.5% HA) achieved in the bulk IPN material, as measured by TGA, with an additional 0.04–0.15% HA added to those samples that were surface dipped (SD). Interestingly, swelling in 0.5 or 1.5% solution resulted in approximately an equivalent amount of HA (0.5 or 1.5%) incorporated into the bulk film, while swelling in the 2.5% solution resulted in only ~1% bulk HA.

Dipping plain LLDPE into HA to coat the surface with HA did not work—the HA layer quickly delaminated from the LLDPE. The IPN treated samples have HA molecules emerging from the surface of the LLDPE with molecular roots that are locked into the LLDPE *via* the IPN structure—the dipping results in a surface layer of HA that is covalently crosslinked to the HA molecules rooted in the HA/LLDPE IPN.

Table 2 indicates a trend towards slightly increased tensile properties in some treatments—some exhibit small, yet significant ( $p < 0.05$ ), increases in yield strength compared to LLDPE-Reference. These materials also exhibited a slight, non-significant trend towards

increases in % $X_c$  with increased %HA, relative to LLDPE-Reference, but there were no statistically significant differences in % $X_c$  between any of the groups tested.

Tensile strength data is not shown in Table 2, but all samples demonstrated considerable strain hardening, as seen in Fig. 2, with ultimate tensile strength equal to breaking strength and not significantly different from the LLDPE-Reference material ( $52.4 \pm 5.2$  MPa).

Although trending slightly higher, bending stiffnesses of all HA/LLDPE IPN films were not significantly different ( $p < 0.05$ ) from those reported in the literature for natural fresh or fixed tissue HV leaflets: fresh leaflet<sup>36</sup> was  $6.3 \pm 2.82$ , fixed leaflet<sup>36</sup> was  $13.87 \pm 8.06$ . Values for the samples tested (all compositions in Table 1) ranged from  $12.93 \pm 2.34$  to  $26.11 \pm 3.62$  nN m<sup>2</sup>. There were no significant differences in bending stiffness between the various compositions.

**Hemocompatibility**—The next figures combine the whole blood clotting and contact angle results. Figure 3 shows results for all samples without the additional HA surface dip and Fig. 4 shows results for all the dipped samples. All HA/LLDPE IPNs (undipped and dipped) exhibit significantly ( $p < 0.05$ ) lower contact angles than LLDPE-Reference material. Furthermore, all HA/LLDPE IPNs cause significantly ( $p < 0.05$ ) less whole blood clotting than the LLDPE-Reference material at both 30 and 60 min; the two lowest contact angles coinciding with the best blood clotting results.

Scanning electron microscopy (SEM) of these samples (Fig. 5) showed considerable thrombus formation on LLDPE-Reference with slightly less thrombus formation on the 0.5% HA samples and considerably less to none on the 1.0% HA and 1.5% HA samples.

Adhesion and activation of human platelets were investigated on LLDPE-Reference and LLDPE + 1.0% HA stained with calcein-AM after 2 h of incubation. Average cell counts were 652 cells/mm<sup>2</sup> (standard deviation 183) on LLDPE-Reference samples and 305 cells/mm<sup>2</sup> (standard deviation 86) on LLDPE + 1.0% HA. Representative SEM images in Fig. 6 show reduced cell adhesion on the LLDPE + 1.0% HA sample compared to LLDPE-Reference. Figure 7 quantifies distribution of adhered platelets exhibiting unactivated and activated dendritic morphology as determined from all SEM images, showing that platelet activation is much lower on LLDPE + 1.0% HA than on LLDPE-Reference.

Representative frames from the high-speed video visualization of valve leaflet motion are shown in Fig. 8, which shows exemplary frames/snapshots from high-speed video studies of these valves in the closed and open configuration under physiological loading in the left heart simulator. Figure 9 shows ensemble averaged flow rate waveforms. The valve with the least regurgitation (LLDPE + 1.5% HA + surface-dip) showed only  $4.77 \pm 0.42\%$  of the forward flow regurgitating during diastole. The corresponding regurgitant volume was  $4.6 \pm 0.4$  mL/beat. For all the valves measured, the EOA was in the range  $2.34 \pm 0.5$  cm<sup>2</sup>.

## DISCUSSION

The fact that the samples swollen in the highest concentration (2.5%) silylHA-CTA/xylene solution had less HA in the final bulk composition than samples swollen in the lower concentration (1.5%) solution is most likely explained by the high viscosity of the 2.5% solution, which hampers diffusion into the swollen LLDPE. This may indicate that these samples (HA/LLDPE + 1.0% HA with and without surface dip) did not reach equilibrium with regard to silylHA-CTA diffusion. Results in Table 1 and Figs. 2 and 3 indicate the optional surface dip resulted in inconsistent amounts of HA applied to the surface. After samples were dipped in the aqueous HA solution for the surface dip process, they were



removed from the aqueous HA solution and hung horizontally in a vacuum oven in an attempt to prevent the HA attaching to the drying surface. However the apparatus used to hang the samples allowed the films to droop so that droplets of the HA solution collected at the low points of the film, resulting in higher HA concentrations in low places and lower HA concentrations at the high points. This consequently prevented a uniform application of HA to the surface. Future work will improve this process and will use Toluidine Blue staining and SEM to examine the uniformity of the surface dip on both sides of the sample.

Preliminary work<sup>12</sup> found that excessive swelling time and temperatures resulted in annealing of the LLDPE crystalline structure and concomitant increases in % $X_c$  and tensile modulus. Swelling parameters used in this study were chosen to minimize these effects. Yet, there were still some slight increases in tensile properties in some samples. These changes were associated with slight trends (not statistically significant) in increases in % $X_c$ . It is also possible that the density of tie molecules between crystalline regions is increasing during the swelling process, which could explain the increases in yield strength and modulus without increases in crystallinity. Even with these slight increases in tensile properties, the bending stiffnesses of the IPN materials did not differ significantly from natural HV tissue. However, the IPN materials did trend towards higher bending stiffnesses.

Interestingly, it is not the HA/LLDPE IPN with the highest HA content, but rather the HA/LLDPE + 1.0% HA + surface-dip sample (Fig. 3) which shows the least clotting. No significant difference was observed between these samples in the amount of free hemoglobin in unclotted blood (gray shaded area). The HA/LLDPE + 1.0% HA samples without the surface dip also showed very little clotting. As mentioned above, the HA/LLDPE + 1.0% HA samples were made with a 2.5% silylHA-CTA swelling solution that was highly viscous and therefore may have resulted in a higher concentration of HA near the outer surface of the LLDPE even though it had less HA overall in the bulk. Future studies will examine the concentration of HA throughout the bulk of the IPN materials and examine intermediate swelling solution concentrations.

The HA/LLDPE + 1.0% HA samples exhibited enhanced anti-thrombogenic properties. Future studies will investigate whether this is due at least in part to the HA being concentrated nearer the surface of the HA/LLDPE + 1.0% HA material than it is in the HA/LLDPE + 1.5% HA samples, possibly due to the relatively high viscosity of the 2.5% silylHA-CTA solution.

Given the inconsistency of the final surface dip, undipped samples were used for this work. The HA/LLDPE + 1.0% HA treatment was chosen for further platelet studies because it produced the best clotting results as well as 53% decrease in cell adhesion on 1.0% HA treated samples as compared to LLDPE-Reference samples. This decrease is likely due to anti-thrombogenic properties and hydrophilic nature of HA as well as the widely accepted notion that most hydrophobic synthetic polymers such as LLDPE are not very hemocompatible.<sup>38</sup> Furthermore, platelet activation results indicate LLDPE-Reference had higher number of activated platelets as compared to LLDPE + 1.0% HA. To bring into context the relevance of these platelet results, similar published results<sup>17,34</sup> for conventional heart valve leaflet materials show that although bioprosthetic (i.e., fixed tissue) HV leaflets are more hemocompatible than mechanical valve leaflets (i.e., pyrolytic carbon), both materials still result in platelet adhesion and activation. Figure 6b shows that the HA/LLDPE IPN elicits almost no platelet adhesion compared to results published elsewhere,<sup>17,34</sup> while the LLDPE-Reference does. Tsai *et al.*'s<sup>34</sup> polyethylene results are very similar to our LLDPE-Reference results (Fig. 5a), and pyrolytic carbon clearly results in more platelet adhesion than our HA/LLDPE (Fig. 5b). Finally, prior study of platelet adhesion on fixed pericardium and fixed pericardium treated with heparin<sup>34</sup> shows that

neither of these materials is as resistant to platelet adhesion as the HA/LLDPE IPN tested in the current study. These results should be directly comparable because both Tsai's and Goodman's polyethylene results are similar to the current study, but the current study used more than double the incubation time. Tsai *et al.*<sup>34</sup> used an incubation time of 1 h and Goodman<sup>17</sup> used 45 min, both less than our 2 h incubation time. Longer incubation time is preferable to allow adequate cell adhesion. It appears that HA/LLDPE IPN materials are at least as hemocompatible (as measured by platelet activity) as fixed tissues commonly used in THVs (even those with attached surface heparin), if not more so.

The HA/LLDPE IPN materials were used to make a trileaflet HV that was tested in a pulsatile flow loop system. Our results show promising hemodynamic performance. Regurgitant volume was  $4.6 \pm 0.4$  mL/beat for the best performing valve, which is slightly above the range for stented bioprostheses but well below that of mechanical valves.<sup>41</sup> For all valves measured, EOA was in the range  $2.34 \pm 0.5$  cm<sup>2</sup>. This is considered excellent as it exceeds most of the stented bioprosthetic valves, which have an EOA < 2 cm<sup>2</sup> for the same valve size.<sup>41</sup> As described above, the bending stiffness of the HA/LLDPE IPN materials trended higher than natural heart valve leaflet. Decreasing this by using thinner film and/or lower modulus films may further improve hemodynamic performance.

Further study will be required to further characterize this material in terms of compositional profile throughout the cross-sectional area, and properties critical to performance in heart valve applications, such as durability, and resistance to calcification.

## CONCLUSIONS

The goal of this research was to create HA/LLDPE IPN materials for flexible heart valve leaflets that exhibit reduced thrombus formation and platelet activation relative to unmodified LLDPE and common HV materials. Hyaluronan was introduced into LLDPE through solvent infiltration by exploitation of the swelling kinetics of the materials. In xylenes solution, silylated HA-CTA quickly diffused into the film of the LLDPE film, so the treatment process was fast and simple. The treatment process enabled composition control and did not notably alter the mechanical properties of the LLDPE. Future work will investigate a more complete range of swelling solution concentrations to determine whether anti-thrombogenicity can be further enhanced.

The presence of HA within the HA/LLDPE IPNs reduced the static water contact angles for all LLDPE samples. An additional dip coating of HA resulted in non-uniform distribution of HA on the surface of LLDPE. All HA/LLDPE samples showed less clotting than LLDPE-Reference material. HA/LLDPE + 1.0%HA materials showed considerably less platelet adhesion and activation than LLDPE-Reference and conventional HV materials (e.g., fixed tissue, pyrolytic carbon).

Trileaflet HVs made with HA/LLDPE materials exhibited excellent hemodynamics, on par with THVs, warranting further investigation and development of these HA/LLDPE IPN materials for use in flexible HV leaflets.

## Acknowledgments

Research reported in this publication was supported by the Colorado Office of Economic Development and International Trade, Bioscience Discovery Evaluation Grant Program, and by the National Institutes of Health National Heart, Lung and Blood Institute under Award Number R01HL119824. The content is solely the responsibility of the authors and does not necessarily represent the official views of the State of Colorado or the National Institutes of Health.

## References

1. ASTM. Standard Test Method for Stiffness of Fabrics. D1388-08. ASTM International; West Conshohocken, PA: 2012.
2. ASTM. Standard Test Method for Tensile Properties of Thin Plastic Sheeting. D882-12 ASTM International; West Conshohocken, PA: 2012.
3. ASTM. Standard Test Method for Transition Temperatures and Enthalpies of Fusion and Crystallization of Polymers by Differential Scanning Calorimetry. D3418-12. ASTM International; West Conshohocken, PA: 2012.
4. Baudet EM, Puel V, et al. Long-term results of valve replacement with the St-Jude Medical Prosthesis. *J Thorac Cardiovasc Surg.* 1995; 109(5):858–870. [PubMed: 7739245]
5. Bjorck CG, Bergqvist D, Esquivel CO, Larsson R, Rudsvik Y. In vitro evaluation of a biologic graft surface—effect of treatment with conventional and low-molecular weight (LMW) heparin. *Thromb Res.* 1984; 35(6):653– 663. [PubMed: 6506022]
6. Black, MM.; Drury, PJ. *Current Topics in Pathology.* Springer-Verlag; Berlin Heidelberg: 1994. Mechanical and Other Problems of Artificial Valves.
7. Boddohi S, Kipper MJ. Engineering Nanoassemblies of Polysaccharides. *Adv Mater.* 2010; 22(28): 2998–3016. [PubMed: 20593437]
8. Butany J, Ahluwalia MS, Munroe C, Fayet C, Ahn C, Blit P, Kepron C, Cusimano RJ, Leask RL. Mechanical heart valve prostheses: identification and evaluation (erratum). *Cardiovasc Pathol.* 2003; 12(6):322–344. [PubMed: 14630298]
9. Daebritz SH, Fausten B, Hermanns B, Schroeder J, Groetzner J, Autschbach R, Messmer BJ, Sachweh JS. Introduction of a flexible polymeric heart valve prosthesis with special design for aortic position. *Eur J Cardiothorac Surg.* 2004; 25(6):946–952. [PubMed: 15144993]
10. Daebritz SH, Sachweh JS, Hermanns B, Fausten B, Franke A, Groetzner J, Klosterhalfen B, Messmer BJ. Introduction of a flexible polymeric heart valve prosthesis with special design for mitral position. *Circulation.* 2003; 108(10):134–139.
11. Dasi LP, Simon HA, Sucusky P, Yoganathan AP. FLUID MECHANICS OF ARTIFICIAL HEART VALVES. *Clin Exp Pharmacol Physiol.* 2009; 36(2):225–237. [PubMed: 19220329]
12. Dean, HC. Development of a Biopoly™ Micro-composite For Use In Prosthetic Heart Valve Replacements. Fort Collins: Colorado State University, Master of Science; 2011.
13. Ellis JT, Healy TM, et al. Velocity measurements and flow patterns within the hinge region of a Medtronic Parallel(™) bileaflet mechanical valve with clear housing. *J Heart Valve Dis.* 1996; 5(6):591–599. [PubMed: 8953436]
14. Forleo M, Dasi L. Effect of hypertension on the closing dynamics and lagrangian blood damage index measure of the B-Datum Regurgitant Jet in a bileaflet mechanical heart valve. *Ann Biomed Eng.* 2013;1–13.10.1007/s10439-013-0896-1
15. Ghanbari H, Kidane AG, Burriesci G, Ramesh B, Darbyshire A, Seifalian AM. The anti-calcification potential of a silsesquioxane nanocomposite polymer under in vitro conditions: potential material for synthetic leaflet heart valve. *Acta Biomater.* 2010; 6(11):4249–4260. [PubMed: 20601232]
16. Ghanbari H, Viatge H, Kidane AG, Burriesci G, Tavakoli M, Seifalian AM. Polymeric heart valves: new materials, emerging hopes. *Trends Biotechnol.* 2009; 27(6):359– 367. [PubMed: 19406497]
17. Goodman SL. Sheep, pig, and human platelet-material interactions with model cardiovascular biomaterials. *J Biomed Mater Res.* 1999; 45(3):240–250. [PubMed: 10397982]
18. Grande-Allen KJ, Calabro A, Gupta V, Wight TN, Hascall VC, Vesely I. Glycosaminoglycans and proteoglycans in normal mitral valve leaflets and chordae: association with regions of tensile and compressive loading. *Glycobiology.* 2004; 14(7):621–633. [PubMed: 15044391]
19. Han DK, Park K, Park KD, Ahn KD, Kim YH. In vivo biocompatibility of sulfonated PEO-grafted polyurethanes for polymer heart valve and vascular graft. *Artif Organs.* 2006; 30(12):955–959. [PubMed: 17181836]

20. James, SP.; Dean, H., IV; Dasi, LP.; Forleo, MH.; Popat, KC.; Lewis, NR. Glycosaminoglycan and Synthetic Polymer Materials for Blood-contacting Applications. WIPO# WO. 2013/138240-A1. Sep 19. 2013
21. James, SP.; Oldinski, RK.; Zhang, M.; Schwartz, H. Chapter 18: UHMWPE/hyaluronan microcomposite biomaterials. In: Kurtz, S., editor. UHMWPE Handbook. 2. New York: Elsevier; 2009.
22. Kidane AG, Burriesci G, Edirisinghe M, Ghanbari H, Bonhoeffer P, Seifalian AM. A novel nanocomposite polymer for development of synthetic heart valve leaflets. *Acta Biomater.* 2009; 5(7):2409–2417. [PubMed: 19497802]
23. Kito H, Matsuda T. Biocompatible coatings for luminal and outer surfaces of small-caliber artificial grafts. *J Biomed Mater Res.* 1996; 30(3):321–330. [PubMed: 8698695]
24. Lee JH, Lee HB. Platelet adhesion onto wettability gradient surfaces in the absence and presence of plasma proteins. *J Biomed Mater Res.* 1998; 41(2):304–311. [PubMed: 9638536]
25. Leo HL, Dasi LP, Carberry J, Simon HA, Yoganathan AP. Fluid dynamic assessment of three polymeric heart valves using particle image velocimetry. *Ann Biomed Eng.* 2006; 34(6):936–952. [PubMed: 16783650]
26. MatWeb. Material Property Data. n.d. Retrieved from <http://www.matweb.com/>
27. Mohammadi H, Mequanint K. Prosthetic aortic heart valves: modeling and design. *Med Eng Phys.* 2011; 33(2):131–147. [PubMed: 20971672]
28. Oosthuysen A, Zilla PP, Human PA, Schmidt CAP, Bezuidenhout D. Bioprosthetic tissue preservation by filling with a poly(acrylamide) hydrogel. *Biomaterials.* 2006; 27(9):2123–2130. [PubMed: 16263164]
29. Sacks MS, Yoganathan AP. Heart valve function: a biomechanical perspective. *Philos Trans R Soc B Biol Sci.* 2007; 362(1484):1369–1391.
30. Simon HA, Dasi LP, Leo HL, Yoganathan AP. Spatio-temporal flow analysis in bileaflet heart valve hinge regions: potential analysis for blood element damage. *Ann Biomed Eng.* 2007; 35(8): 1333–1346. [PubMed: 17431789]
31. Smith BS, Yoriya S, Grissom L, Grimes CA, Popat KC. Hemocompatibility of titania nanotube arrays. *J Biomed Mater Res, Part A.* 2010; 95A(2):350–360.
32. Tan QG, Ji J, Barbosa MA, Fonseca C, Shen JC. Constructing thromboresistant surface on biomedical stainless steel via layer-by-layer deposition anticoagulant. *Biomaterials.* 2003; 24(25): 4699–4705. [PubMed: 12951013]
33. Thorslund S, Sanchez J, Larsson R, Nikolajeff F, Bergquist J. Bioactive heparin immobilized onto microfluidic channels in poly(dimethylsiloxane) results in hydrophilic surface properties. *Colloids Surf B Biointerfaces.* 2005; 46(4):240–247. [PubMed: 16352425]
34. Tsai CC, Chang Y, Sung HW, Hsu JC, Chen CN. Effects of heparin immobilization on the surface characteristics of a biological tissue fixed with a naturally occurring crosslinking agent (genipin): an in vitro study. *Biomaterials.* 2001; 22(6):523–533. [PubMed: 11219715]
35. Unger F, Ghosh P. International cardiac surgery. *Semin Thorac Cardiovasc Surg.* 2002; 14(4):321–323. [PubMed: 12652432]
36. Vesely I, Boughner D. Analysis of the bending behavior of porcine xenograft leaflets and of natural aortic valve material—bending stiffness, neutral axis and shear measurements. *J Biomech.* 1989; 22(6–7):655–671. [PubMed: 2509479]
37. Wang YX, Robertson JL, Spillman WB, Claus RO. Effects of the Chemical Structure and the Surface Properties of Polymeric Biomaterials on Their Biocompatibility. *Pharm Res.* 2004; 21(8): 1362–1373. [PubMed: 15359570]
38. Werner C, Maitz MF, Sperling C. Current strategies towards hemocompatible coatings. *J Mater Chem.* 2007; 17(32):3376–3384.
39. Wu KK, Thiagarajan P. Role of endothelium in thrombosis and hemostasis. *Annu Rev Med.* 1996; 47:315–331. [PubMed: 8712785]
40. Yacoub M, Takkenberg J. Will heart valve tissue engineering change the world? *Nat Clin Pract Cardiovasc Med.* 2005; 2(2):60–61. [PubMed: 16265355]
41. Yoganathan AP, He ZM, Jones SC. Fluid mechanics of heart valves. *Annu Rev Biomed Eng.* 2004; 6:331–362. [PubMed: 15255773]

42. Zhang M, James SP, Rentfrow E. The effect of IPN treatment on the mechanical properties of UHMWPE. *Biomed Sci Instrum.* 2001; 37:7–12. [PubMed: 11347448]
43. Zhang M, King R, Hanes M, James SP. A novel ultra high molecular weight polyethylene–hyaluronan microcomposite for use in total joint replacements. I. Synthesis and physical/chemical characterization. *J Biomed Mater Res A.* 2006; 78A(1):86–96. [PubMed: 16602125]
44. Zhang M, King R, Hanes M, James SP. A novel ultra high molecular weight polyethylene–hyaluronan microcomposite for use in total joint replacements. II. Mechanical and tribological property weight composite for evaluation. *J Biomed Mater Res A.* 2007; 82A(1):18–26. [PubMed: 17265440]
45. Zilla P, Brink J, Human P, Bezuidenhout D. Prosthetic heart valves: catering for the few. *Biomaterials.* 2008; 29(4):385–406. [PubMed: 17950840]

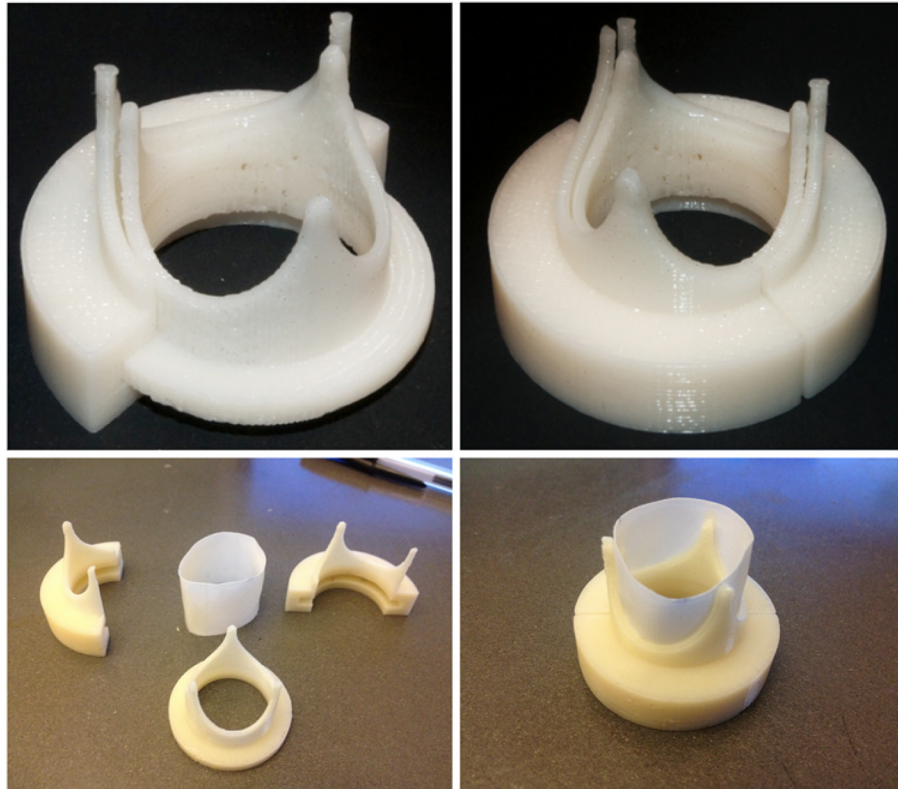


**FIGURE 1.**  
3D printed heart valve assembly for leaflets composed of a cylindrical section of material.

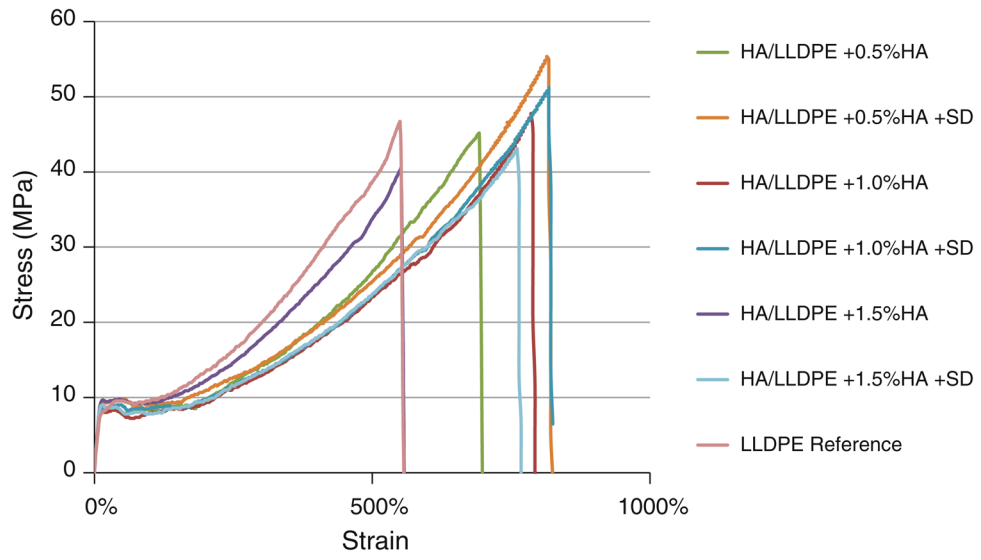


**FIGURE 2.** Representative stress–strain plots of each treatment, all demonstrating strain hardening.

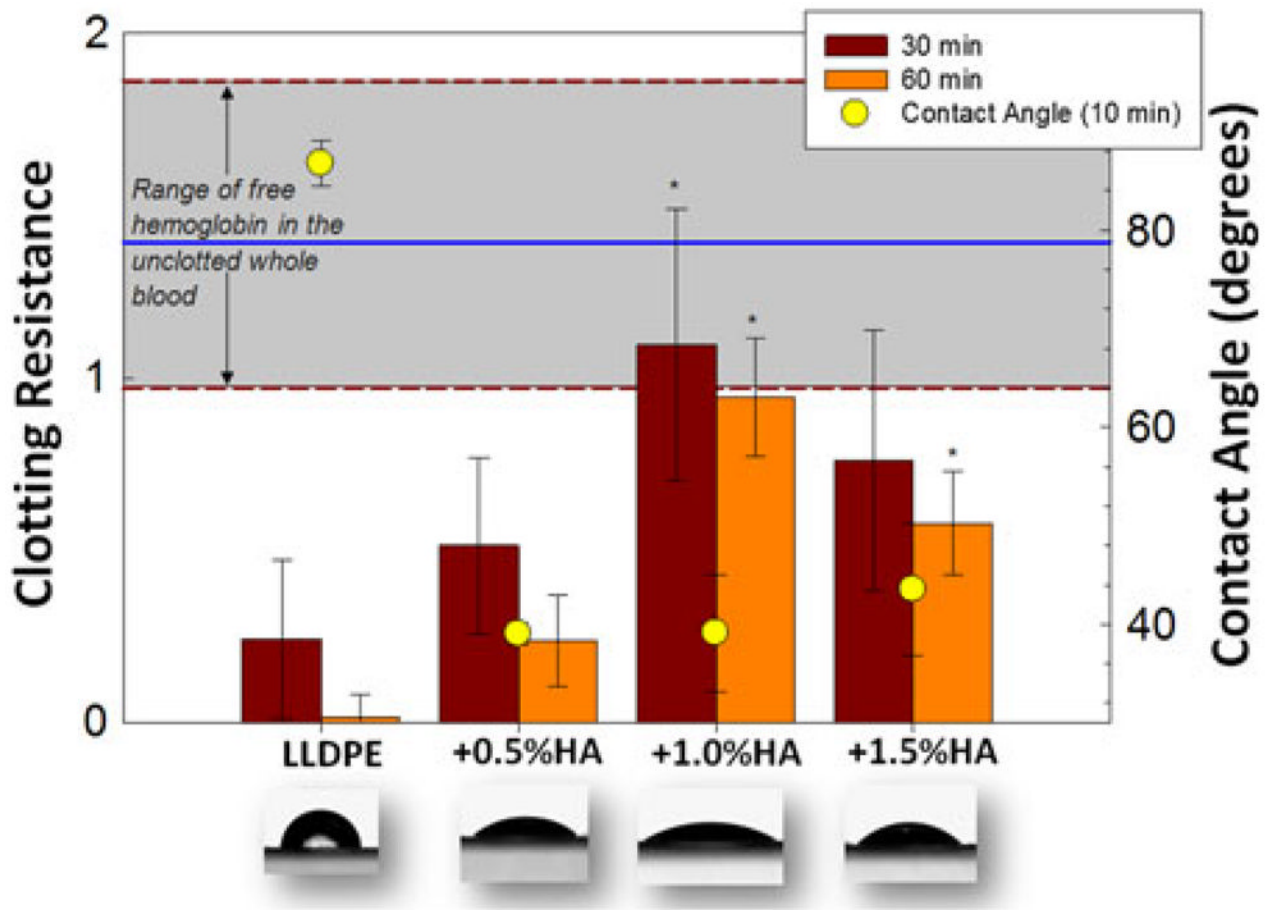


**FIGURE 3.** Clotting resistance on left axis (free hemoglobin absorbance) for non-dipped samples for the 30 min and 60 min time points (—:  $\bar{x}$ , - - -:  $\pm\sigma$  shaded gray for unclotted blood). Contact angles (right axis) and overlaid images 10 min after drop application. \*Significant differences ( $p < 0.05$ ) from the LLDPE-Reference.



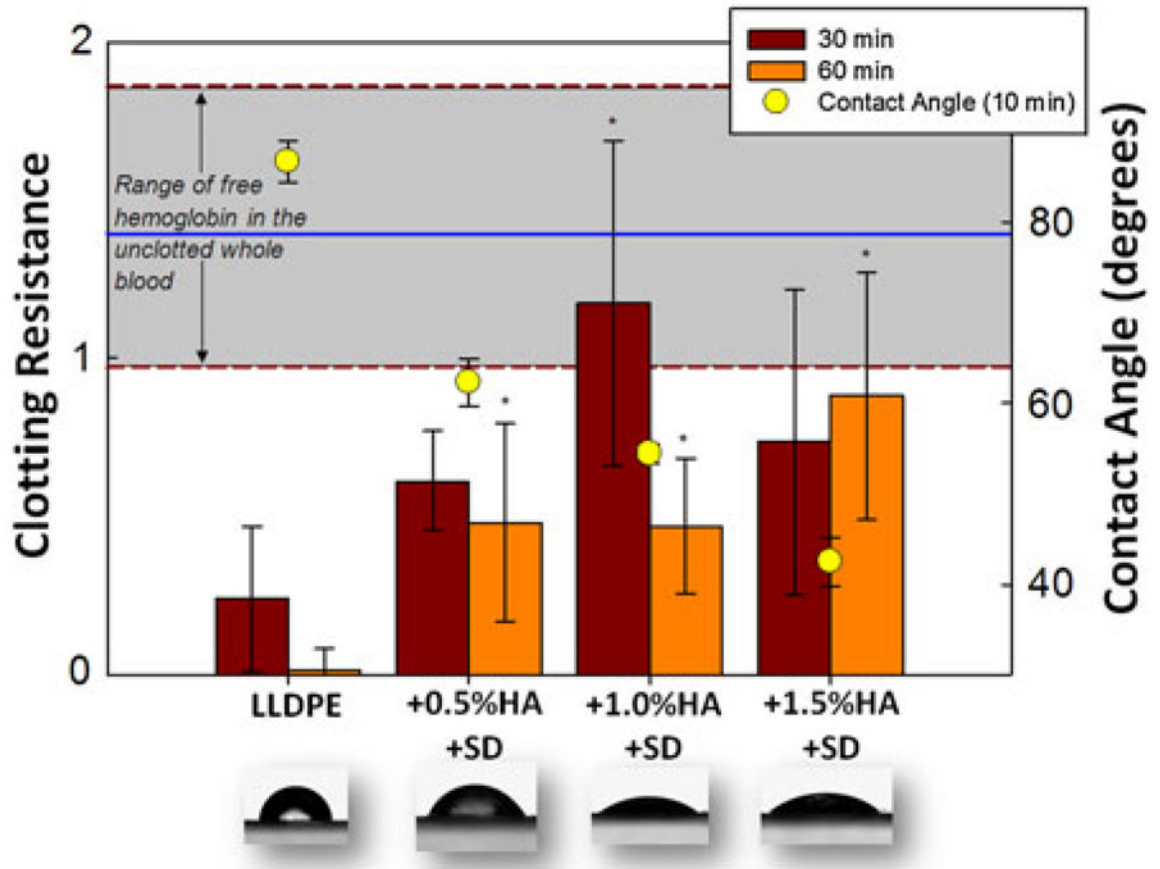


**FIGURE 4.** Same description as Fig. 3, but for HA dipped samples.

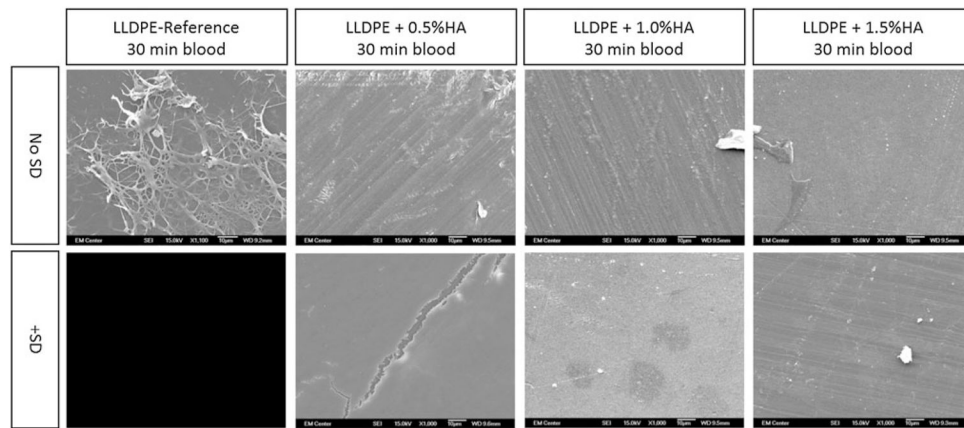


**FIGURE 5.** SEM images (all 1000 $\times$ ) of HA/LLDPE with and without surface dip samples for all concentrations, after being contacted with whole blood for 30 min, clearly showing that the surface of unmodified LLDPE-Reference samples were covered with an accumulation of fibrin and thrombus, while those with HA/LLDPE showed almost no sign of thrombus formation.

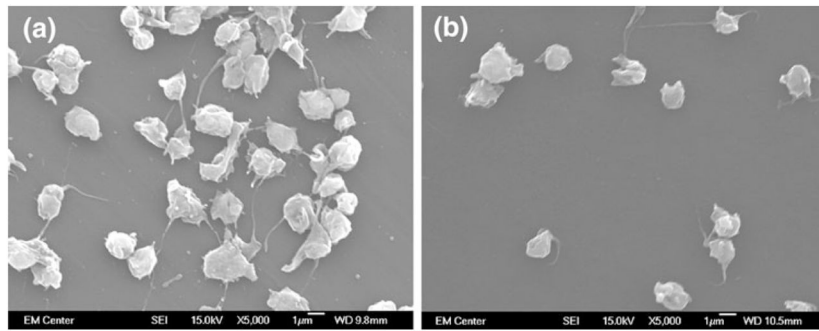


**FIGURE 6.** Representative platelet adhesion and activation on LLDPE-Reference (a) and HA/LLDPE + 1% HA (b).

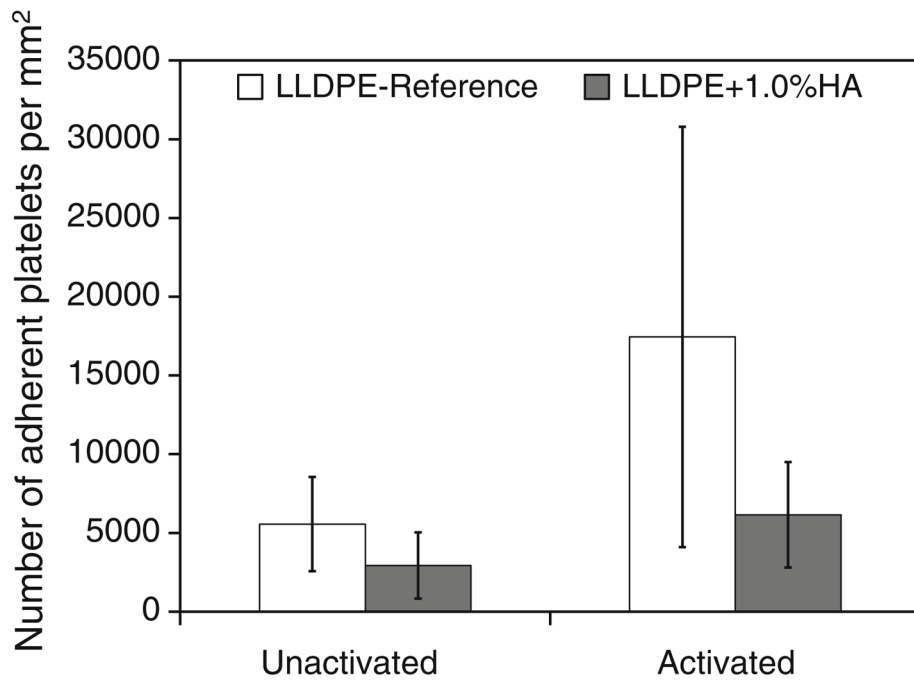


**FIGURE 7.** Distribution of adhered platelets exhibiting unactivated and activated dendritic morphology on LLDPE-Reference and HA/LLDPE + 1% HA materials.

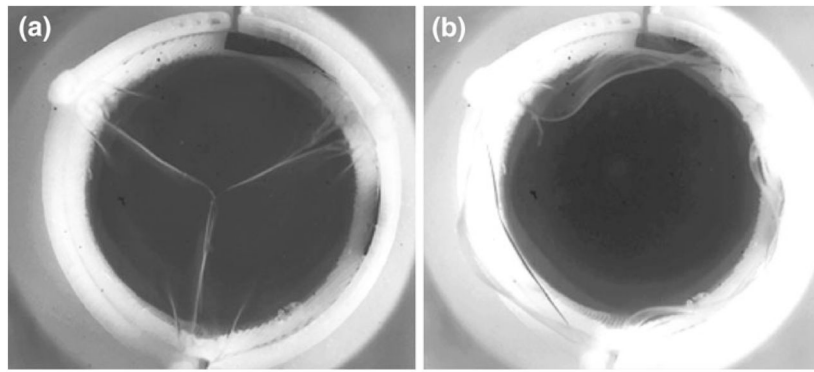


**FIGURE 8.** Single frame of high-speed (1000 fps) leaflet kinematics study of HV with HA/LLDPE + 1% HA leaflets in the aortic position during diastole (a) and systole (b).

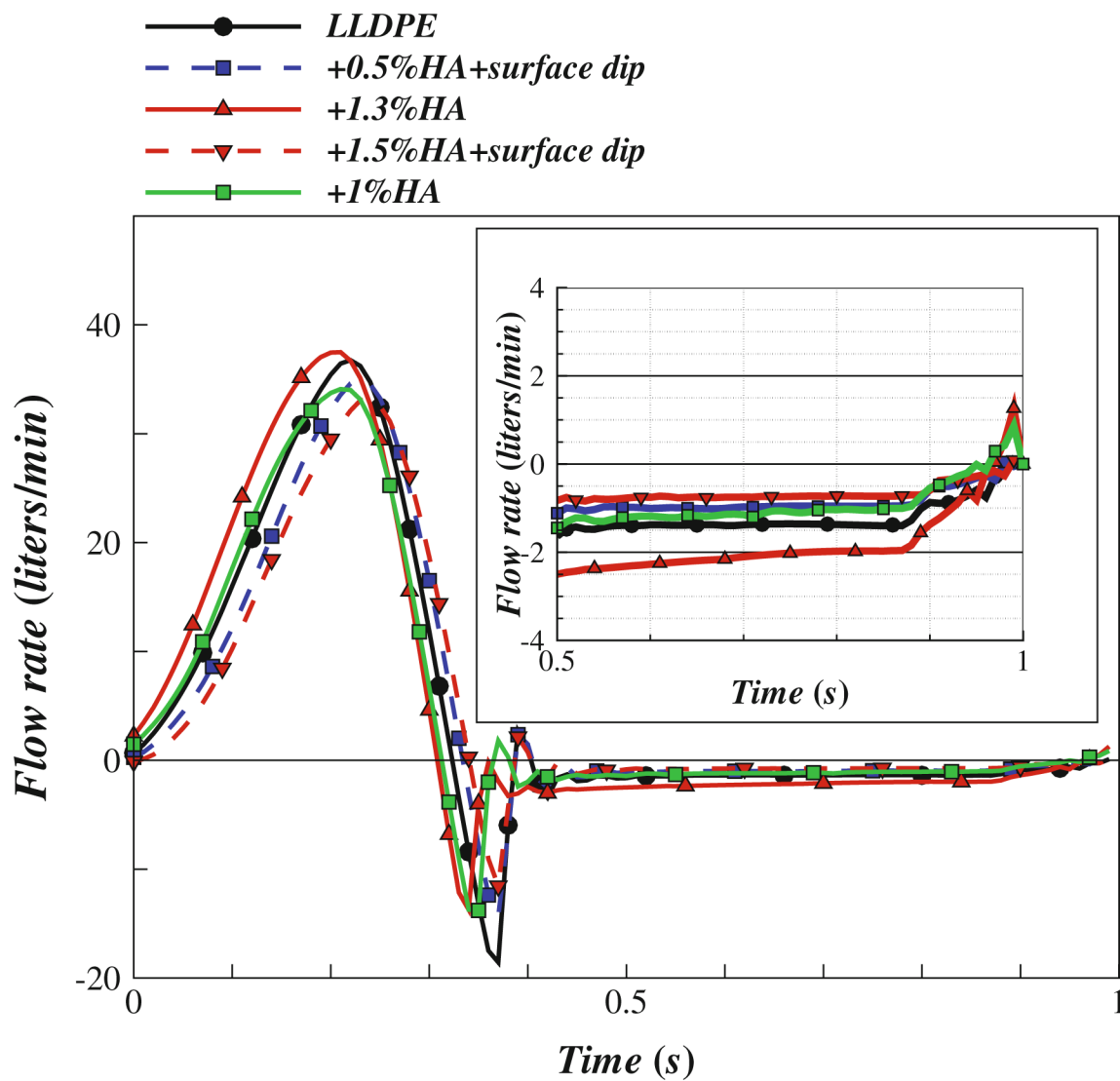


**FIGURE 9.** Measured flow rate curves for the tested HVs under mean aortic pressure of 100 mmHg and cardiac output of about 5 L/min, with a zoomed-in view of the regurgitation portion of the flow curve.

**TABLE 1**

Swelling solution concentrations used, actual composition of samples and sample names used throughout the study.

SilylHA-CTA/xylenes swell. soln. conc. (g/100 mL)	Actual <sup>a</sup> bulk weight % HA (w/w)	Actual <sup>a</sup> surface Weight % HA (w/w)	Sample name
n.a.	n.a.	n.a.	LLDPE-Reference
0.5	0.507 ± 0.01	n.a.	HA/LLDPE + 0.5% HA
2.5	1.00 ± 0.07	n.a.	HA/LLDPE + 1.0% HA
1.5	1.32 ± 0.18	n.a.	HA/LLDPE + 1.5% HA
0.5	0.542 ± 0.05	0.035 ± 0.01	HA/LLDPE + 0.5% HA + SD
2.5	1.05 ± 0.22	0.043 ± 0.01	HA/LLDPE + 1.0% HA + SD
1.5	1.47 ± 0.37	0.146 ± 0.01	HA/LLDPE + 1.5% HA + SD

<sup>a</sup>Determined by TGA.

“+1.5%” used in name for consistency with SD samples even though actual composition was +1.3%.

SD optional surface dip applied.

TABLE 2

Mechanical properties and % $X_c$  of various HA/LLDPE IPN materials.

	Modulus (MPa)	Yield strength (MPa)	% Elongation	% $X_c$	Bending stiffness (nN m <sup>2</sup> )
LLDPE-Reference	73.82 ± 6.83	7.29 ± 0.29	582 ± 23	28.14 ± 2.36	26.10 ± 3.62
HA/LLDPE + 0.5% HA	76.49 ± 1.86	8.23 ± 0.33*	787 ± 76	32.97 ± 1.07	19.81 ± 5.90
HA/LLDPE + 1.0% HA	84.05 ± 15.30	8.59 ± 0.90*	755 ± 75	32.66 ± 2.31	17.21 ± 5.22
HA/LLDPE + 1.5% HA	99.71 ± 12.62*	9.74 ± 0.61*	476 ± 85	30.13 ± 1.88	21.72 ± 5.07
HA/LLDPE + 0.5% HA + SD	81.56 ± 4.44	8.61 ± 0.30*	757 ± 70	31.54 ± 1.12	17.85 ± 5.16
HA/LLDPE + 1.0% HA + SD	85.12 ± 11.01	9.04 ± 0.47*	728 ± 168	31.86 ± 1.59	18.00 ± 4.80
HA/LLDPE + 1.5% HA + SD	89.92 ± 9.64	8.70 ± 0.08*	601 ± 147	31.74 ± 3.01	12.93 ± 2.34

\* Significant difference ( $p < 0.05$ ) from the LLDPE-Reference material.